AB_5-Type Hydrogen Storage Alloys as Catalysts in Hydrogen-Diffusion Electrodes for Novel H_2/Hydride//Perovskite/O_2 Alkaline Fuel Cells

Wei-Kang Hu,[†] Yohannes Kiros,[‡] and Dag Noréus*,[†]

Department of Structural Chemistry, Arrhenius Laboratory, Stockholm University, S-106 91 Stockholm, Sweden, and Department of Chemical Engineering and Technology, Chemical Reaction Engineering, KTH—Royal Institute of Technology, S-100 44, Stockholm, Sweden

Received: June 2, 2004

Development of a non-noble-metal catalyst electrode is an important issue in the research and development of fuel cells. The catalytic activity and durability of AB_5-type hydrogen storage alloys used in hydrogen-diffusion electrodes for alkaline fuel cells are evaluated. The experiments demonstrate that the activity and stability for hydrogen oxidation is greatly improved if the particle size is decreased from 5−30 to 1−10 μm. This also improves the electrode stability. SEM and XRD analyses show that no disintegration of the smaller catalyst particles is observed in long-term tests. A novel H_2/hydride//perovskite/O_2 alkaline fuel cell was constructed as a non-noble-metal fuel cell concept. The results showed that both gas-diffusion electrodes had high catalytic activities and good stability. A maximum power density of 54 mW/cm^2 was achieved at 120 mA/cm^2 when using H_2/O_2 and 49 mW/cm^2 at 100 mA/cm^2 when using H_2/air.

1. Introduction

Fuel cells for mobile applications have attracted much attention because of their high efficiencies and low emissions.[1] The use of noble metals (particularly platinum) and their alloys as catalysts in low-temperature fuel cells (such as proton exchange membrane fuel cells, direct methanol fuel cells, phosphoric acid fuel cells) limits, however, their possibility of becoming a common power source for the future world automobile market.[2,3] Therefore, it is highly desirable to develop platinum-free catalysts. Alkaline fuel cells (AFCs) can today use a non-noble-metal catalyst (e.g., Raney Ni/Ag). However, the high loadings of Raney Ni or Ag do not provide a significant cost advantage over platinum.[1] Therefore, studies on non-Raney Ni/Ag catalysts in the AFC system are of interest. Rare-earth-based AB_5-type hydrogen storage alloys have been extensively investigated as negative electrodes in rechargeable Ni/metal hydride (NiMH) batteries during the past two decades, where their ability to rapidly absorb hydrogen under ambient temperature and pressures has been demonstrated. Recently, rare-earth-based AB_5-type hydrogen storage alloys have been tested as electrode materials in AFCs.[4−6] However, the activity for hydrogen oxidation remains low and the stability needs to be improved. The purpose of this work is to circumvent these drawbacks by reducing particle sizes and optimizing parameters of electrode fabrication. A H_2/hydride//perovskite/O_2 alkaline fuel cell was also constructed, where hydride alloys were evaluated as catalysts in the hydrogen-diffusion electrode and perovskite as a catalyst in the oxygen-diffusion electrode.

2. Experiment

2.1. Preparation of Catalysts and Electrodes. AB_5-type hydrogen storage alloys having a chemical formula of $MmNi_{3.88}$-$Co_{0.85}Mn_{0.39}Al_{0.4}$ were used as catalysts in the hydrogen-diffusion electrode. The alloy powder having particle sizes of 63−90 μm was first treated in a vacuum at a temperature of 280−300 °C for 30 min, then exposed to hydrogen gas at a pressure of 15 atm, and immediately cooled by a water bath. This process was repeated three times. The treatment reduced the alloy powder particle size down to 5−30 μm. The alloy was degassed, and the particle size was further reduced by means of ball milling for 30 min in air. The ball to alloy weight ratio was 15:1. The specific Brunauer−Emmett−Teller (BET) surface area was measured using nitrogen absorption on the degassed catalyst at liquid nitrogen temperatures. After ball milling for 30 min, the catalyst particle size was reduced between 1 and 10 μm and the specific surface area increased to 1.2 m^2/g from 0.6 m^2/g.

The hydrogen-diffusion electrode was fabricated by a rolling method as follows. A mixture was made by blending the alloy particles with a 10 wt % poly(tetrafluoroethylene) (PTFE) solution and carbon black powders having an average particle size of 0.42 μm and a surface area of 80 m^2/g in an argon atmosphere. The weight ratio of the alloy catalyst to carbon black was 9:1. The mixture was then intensively stirred in air to obtain a paste. This paste was rolled to a 0.4 mm thick sheet and then rolled together with a nickel net as a current collector to form a catalyst layer. The catalyst layer was then sintered in hydrogen at 270−290 °C for 8 h. Finally, the hydrogen-diffusion electrode was fabricated by cold-pressing the catalyst layer with a gas diffusion layer at 50−60 kg/cm^2. The gas diffusion layer was a hydrophobic carbon paper sheet with a thickness of 0.38 mm provided by NedStack Fuel Cell Technology BV, The Netherlands. Such a formed hydrogen-diffusion electrode had a thickness of 0.25−0.3 mm with a catalyst loading of 60−80 mg/cm^2.

The catalyst in the oxygen-diffusion electrodes was a perovskite ($La_{0.9}Ca_{0.1}MnO_3$) with an average pore diameter of 58.7 nm, particle sizes in the range of 50−100 nm, and a specific surface area of 35 m^2/g. The oxygen-diffusion electrode was

* To whom correspondence should be addressed. Fax: +46-8-152187. E-mail: dag@struc.su.se.
[†] Stockholm University.
[‡] KTH—Royal Institute of Technology.

10.1021/jp047620x CCC: $27.50
Published on Web 11/06/2004

prepared by the same method as described above. More details about the synthesis of the catalysts and electrode fabrication were described in the literature.[7,8]

2.2. Electrochemical Measurements and Physical Features of Catalysts. The catalytic activities of the gas-diffusion electrodes were evaluated in a single-compartment, three-electrode cell with an electrolyte of 30 wt % KOH at 55 °C. Steady-state current−potential curves of the electrode were measured. The gas-diffusion electrode served as the working electrode. The counter electrode was a platinum foil having an area of 12.5 cm^2, and the reference electrode was a Hg/HgO electrode with the same electrolyte. The electrode stability was examined by employing a constant current density at 55 °C.

For the H_2/hydride//perovskite/O_2 alkaline fuel cell, the electrode potentials were measured with respect to a Hg/HgO reference electrode connected through two small holes near both electrodes. The cell was operated at 55 °C using two modes: (a) H_2/O_2 with a flow rate of 15 mL/min and (b) H_2/air with an airflow rate of 35 mL/min at a pressure of 1.2−1.3 bar. When air was supplied to the cathode, a 6 M NaOH solution was used as a scrubber to remove CO_2. To get the best performance, the hydrogen- and oxygen-diffusion electrodes were immersed in the 30% KOH solution at 55 °C for 24 h prior to operation. Hydrogen and oxygen gases were continuously supplied from the backsides of both electrodes.

After electrochemical tests, the electrodes were removed from the experimental cell and rinsed using distilled water several times. Then, the electrode was divided into several parts for subsequent characterization. The catalyst particle size and surface morphology were observed by scanning electron microscopy (SEM). The chemical compositions on the catalyst layer were analyzed by energy-dispersive X-ray spectroscopy (EDS). A phase analysis was made by powder X-ray diffraction (XRD) using Cu $K\alpha_1$ (1.5406 Å) radiation.

3. Results and Discussion

3.1. Particle Sizes and Activation of Hydrogen-Diffusion Electrodes. The hydrogen-diffusion electrodes need activation treatments before the electrochemical measurements due to passivation of the surface hydride catalysts when exposed to air during electrode fabrication. To reach the best performance, the electrode was activated by cathodic polarization with a current density of 5−20 mA/cm^2 for one to several hours and then using an anodic current density of 15−20 mA/cm^2 for several days. However, it is very important to control the current density and time if electrodes with a catalyst size of more than 10 μm are to be activated by means of cathodic polarization since the larger particles may crack up on hydrogenation. Figure 1a shows the surface morphology of the electrode having a catalyst particle size of 5−30 μm. After cathodic polarization for 20 h at a current density of 10 mA/cm^2, many cracks on the surface of catalysts were noticed and the larger catalyst particles broke up into small parts. This is not our desire as it may hinder hydrogen transport within the cracked particles, leading to performance degradation. The catalyst pulverization is caused by internal stress as the particles expand upon hydrogen absorption.[9] To avoid this, the activation time and the cathodic current density were kept less than 10 h and 10 mA/cm^2, respectively. In contrast, the catalyst pulverization did not occur for small particles less than 10 μm, even at cathodic current densities as high as 40 mA/cm^2 for 20 h because the buildup of internal stress is less[10] (see Figure 1b). Therefore, the particle size of the hydride should be less than 10 μm in order to obtain high stability and good performance even after long activation at high cathodic current densities.

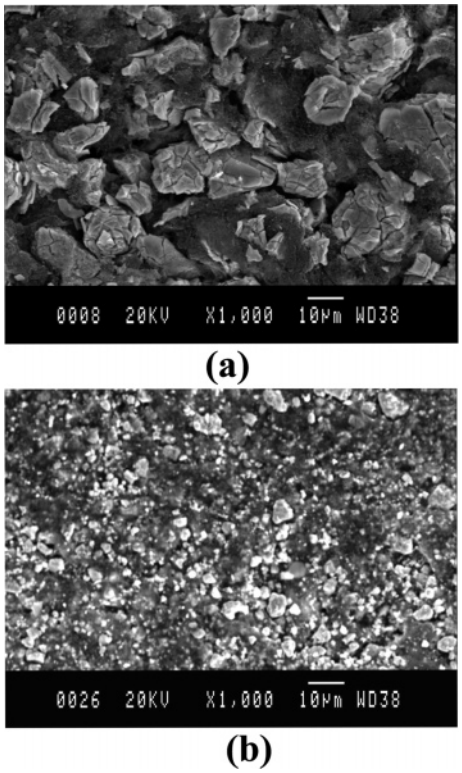

Figure 1. SEM images of hydrogen-catalytic electrodes having a particle size of (a) 5−30 μm and (b) 1−10 μm after cathodic activation.

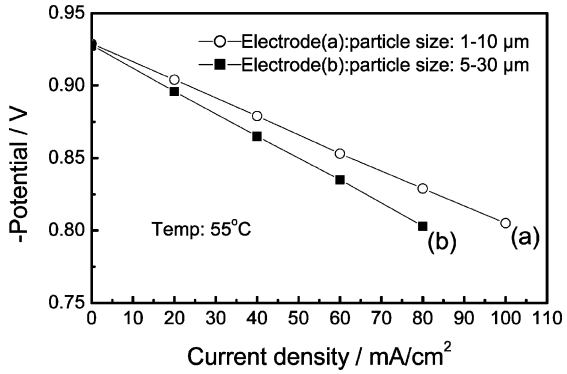

Figure 2. Polarization curves of two hydrogen-diffusion electrodes in 30 wt % KOH at 55 °C.

3.2. Electrochemical Activity and Durability. To compare activities and durability, the hydrogen-diffusion electrodes in this article were made of the two kinds of hydride catalysts with particle sizes of 5−30 and 1−10 μm, respectively. They were activated first by cathodic polarization with a current density of 6 mA/cm^2 for 10 h and consequently by an anodic current density of 20 mA/cm^2 for 100 h. During activation, hydrogen gas was supplied to a gas chamber on the backside of the electrodes. Then, a stable equilibrium hydrogen potential was established at −0.925 V, indicating that the hydrogen molecules were absorbed and dissociated into atoms on the catalyst surface. Figure 2 shows the polarization curves of the two hydrogen-diffusion electrodes. It can be seen that the polarized potential of both electrodes varied almost linearly with the current density. The polarization resistance is estimated to be 1.6 and 1.3 Ω cm^2 at 55 °C, respectively. The electrode with the small particle size catalyst had lower polarization resistance and a higher catalytic activity. However, the polarization resistance was still high, compared to a Pt/Pd catalyst or Raney Ni catalyst, which have polarization resistances of 0.16−0.33

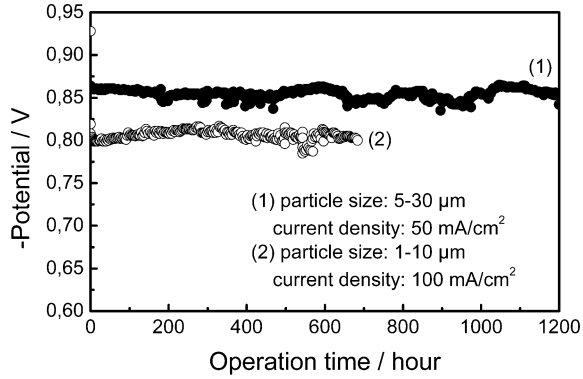

Figure 3. Hydrogen-oxidation potential versus operational time. Curve 1 represents a particle size of 5−30 μm at a current density of 50 mA/cm^2. Curve 2 represents a particle size of 1−10 μm at a current density of 100 mA/cm^2.

Ω cm^2.[11] The higher polarization resistance in our case was thought to be related to the lower specific surface area of the large catalyst particle size, compared to Raney Ni having a specific surface area of ca. 70 m^2/g and a particle size of <2 μm. In addition, the hydrogen diffusion within the hydrogen storage alloys ($D_H = 7-8 \times 10^{-(8-11)}$ cm^2/s)[12] is much lower than that of Pt catalysts ($D_H = 3-5 \times 10^{-5}$ cm^2/s),[13] Pd catalysts ($D_H = 6 \times 10^{-(3-5)}$ cm^2/s),[14] and Ni catalysts ($D_H = 1 \times 10^{-(4-6)}$ cm^2/s).[15] When a low anodic current density is employed, the hydrogen diffusion and particle size have less effect on the performance. As the current density increases, however, the atomic hydrogen at the reaction interface is rapidly consumed and the hydrogen concentration on the surface is significantly reduced. Hydrogen diffusion into the surface layer is probably slow compared to the rate of electrochemical oxidation reactions, leading to a noticeable drop of hydrogen oxidation potential at high anodic current densities. In our experiments, we have observed that the electrode with a large catalyst particle size had a high polarization resistance and could not gain a stable oxidation potential at an anodic current density of more than 70 mA/cm^2. In contrast, the electrode with a relatively small catalyst particle size can achieve a stable hydrogen oxidation potential even at a current density as high as 100 mA/cm^2, as shown in Figure 3 (see curve 2). From these results, we anticipate that the polarization resistance may be significantly reduced and electrochemical performance could be further improved if nanosize hydride particles are used as catalysts in combination with a high surface area carbon since the hydrogen diffusion becomes less limiting for small particles. Also, the catalytic activity increases with a larger specific surface area.

3.3. Composition and Structure of the Catalyst. Figure 4 shows SEM micrographs of both hydrogen-diffusion electrodes after long-term tests (as shown in Figure 3). Both catalysts with different particle sizes were stable, and no pulverization was observed after long-term hydrogen-catalytic oxidation reactions. This indicates good mechanical and electrochemical stability. The chemical composition on the catalytic surface was investigated with EDS. Table 1 presents the chemical composition before and after tests. As seen in Table 1, an increase of rare-earth content on the electrode surface was found after long-time tests. This segregation reflects the relative ease with which rare-earth elements are oxidized in alkaline media. A similar segregation phenomenon has also been observed when rare-earth-based AB_5 alloys are used as the negative electrode in NiMH cells.[16] The segregation also resulted in an A-rich and B-poor stoichiometry, as shown in Table 1. In addition, a small

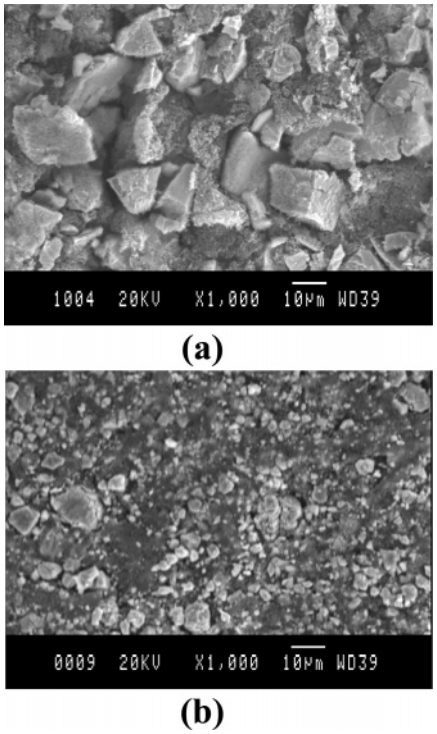

Figure 4. SEM images of the hydrogen-diffusion electrodes after (a) 2200 h at 50 mA/cm^2 and (b) 700 h tests at 100 mA/cm^2.

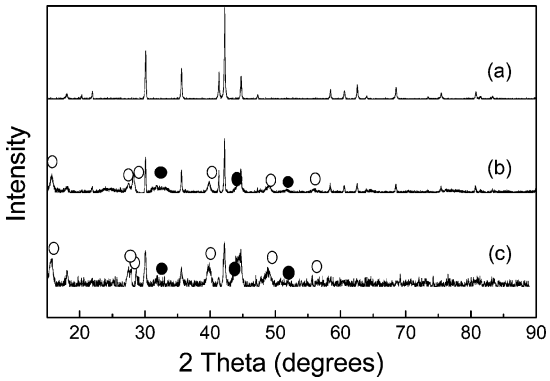

Figure 5. XRD patterns of hydride catalysts (a) before test, (b) after 2200 h at 50 mA/cm^2, and (c) after 700 h tests at 100 mA/cm^2. The peaks marked with white and black spheres correspond to the rare-earth hydroxide and Ni_2O_3 phases, respectively.

TABLE 1: Chemical Composition on the Catalyst Surface before and after Electrochemical Test

element	before test	after 2200 h	element	before test	after 2200 h
La	9.079	10.419	Mn	5.930	6.424
Ce	1.893	2.078	Al	6.659	2.572
Pr	1.470	1.790	Ca	0.000	0.352
Nd	2.799	3.241	S	0.000	0.194
Ni	59.178	59.899	stoichiometry	$AB_{5.56}$	$AB_{4.68}$
Co	12.976	13.031			

amount of impurities such as Ca and S was also found on the catalyst surface, probably originating from the electrolyte and rubber seal, respectively. However, the existence of small amounts of these elements on the electrode surface seemed to have no observable negative effect on the catalytic activity and stability. Figure 5 presents the X-ray diffraction patterns of the catalyst after tests. Some weak additional peaks were observed. These additional peaks could be assigned to a rare-earth hydroxide phase and a small amount of Ni_2O_3 phase, respec-

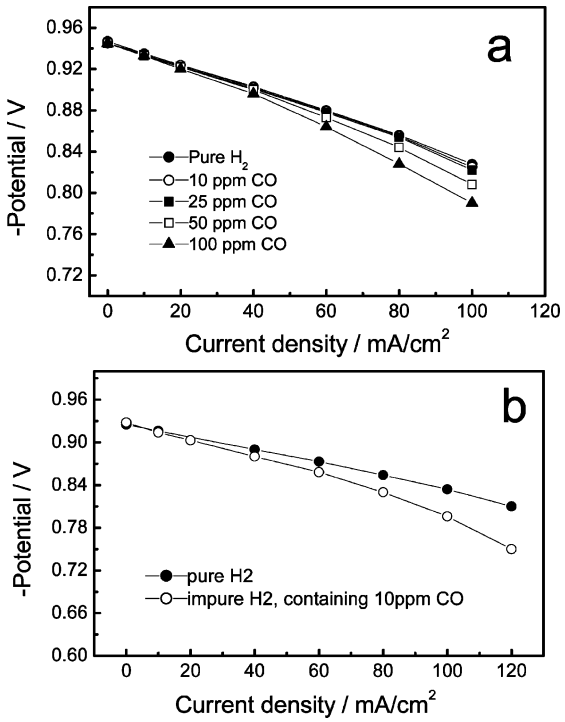

Figure 6. Polarization curves of (a) AB_5-type hydride electrode and (b) Pt-catalyst electrode in 30 wt % KOH at 55 °C using pure and impure H_2.

tively. The formation of rare-earth hydroxide is consistent with the segregation of rare-earth elements on the electrode surface as observed from the EDS analyses.

3.4. Effect of Impure H_2 on the Activity and Stability. Impure hydrogen from the reforming of nature gas, gasoline, or alcohols is a likely fuel source for low-temperature fuel cells. A typical composition of reformed gas is 74% hydrogen, 25% carbon dioxide, and 1−2% carbon monoxide. The content of CO can be reduced down to 10−100 ppm at relatively low cost with catalytic oxidation. But, further reduction increases costs significantly. Pt or its alloys are widely used as catalysts to oxidize hydrogen in low-temperature fuel cells. Pt is, however, easily poisoned by traces of CO, significantly deteriorating the performance at levels as low as 10 ppm CO.[17,18] To examine the effect of small amounts of CO on the activity of hydride catalysts, an impure hydrogen gas containing 10−100 ppm CO was studied. Figure 6a shows the effect of the impure hydrogen gas on the activity of AB_5-type hydride catalysts. For comparison, the performance of a Pt-catalyst electrode is also presented in Figure 6b, where 10 wt % Pt on activated carbon with a particle size of 20−30 μm was employed. The catalytic activity of the Pt-catalyst electrode declined when using an impure hydrogen gas containing 10 ppm CO since CO is adsorbed chemically on the active sites of platinum.[19−22] By comparison, the AB_5-type hydride catalysts had a better CO tolerance, especially below 25 ppm CO. As the CO content increased above 50 ppm, negative effects on the activity were, however, observed.

3.5. Performance of H_2/Hydride//Perovskite/O_2 Alkaline Fuel Cells. The AB_5-type hydride catalysts show high catalytic activities and good stability in a half-cell configuration, especially if the particle size is reduced to 1−10 μm. These results provide us with the opportunity to construct a novel H_2/hydride//perovskite/O_2 alkaline fuel cell and investigate its performance. In our construction of this fuel cell, the hydrogen-diffusion electrode was composed of AB_5-type hydride catalysts

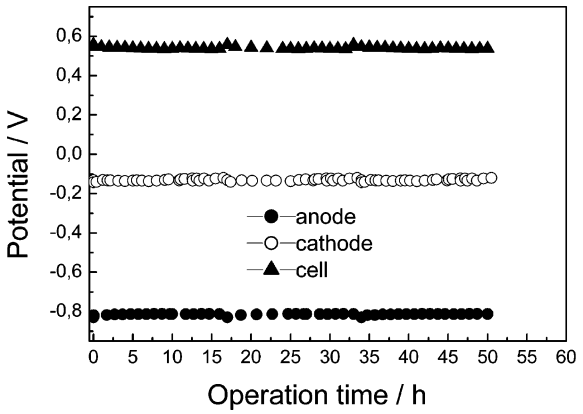

Figure 7. Polarization potential of both gas-diffusion electrodes and voltage of the fuel cell at 100 mA/cm^2.

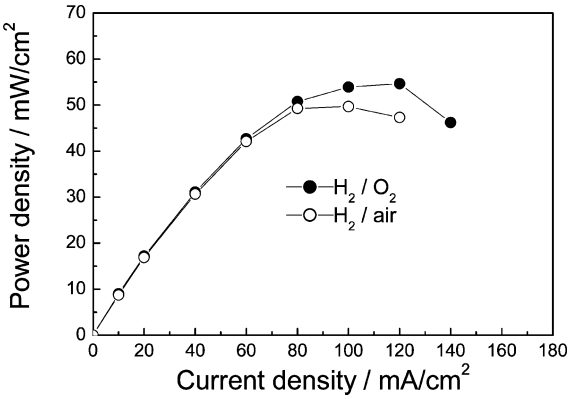

Figure 8. Power densities vs current densities in two cases of H_2/O_2 and H_2/air.

with particle sizes of 1−10 μm, while the oxygen-diffusion electrode was made of a $La_{0.9}Ca_{0.1}MnO_3$ perovskite with particle sizes of 50−100 nm. Each electrode has a geometrical area of 5.0 cm^2 in contact with the electrolyte of 30 wt % KOH. The distance between anode and cathode was 1.2 cm. To stabilize the performance, the cell needs to be activated and conditioned at a low current density of 10−20 mA/cm^2 for at least 50 h before operation at high current densities. Figure 7 shows the polarization potential of both electrodes and cell voltage at current densities of 100 mA/cm^2 and 55 °C using H_2 in the anode and O_2 in the cathode, respectively. The hydrogen- and oxygen-diffusion electrodes showed good activities and stabilities. Figure 8 presents the power densities versus current densities. As seen in Figure 8, a maximum power density of 54 mW/cm^2 was achieved at 120 mA/cm^2 in the case of pure H_2/O_2. When using air instead of pure oxygen, the maximum power density of 49 mW/cm^2 was obtained at 100 mA/cm^2. A higher power density could be expected by shortening the distance between the anode and cathode to lower the ohmic losses of electrolyte.

4. Conclusion

AB_5-type hydrogen storage alloys with two different particle sizes were used as catalysts to compose hydrogen-diffusion electrodes. The hydrogen-diffusion electrodes for hydrogen absorption−oxidation were investigated. This type of hydrogen-diffusion electrode showed a good activity as well as stability. Use of small particles increases the specific surface area and reduces the hydrogen-diffusion pathway within the catalyst particles, increasing the catalytic activity and allowing for anodic current densities up to 100 mA/cm^2. Further improvement of

performance is possible if still smaller hydride catalysts are developed and if the electrode structure and composition are further optimized. In this work, we also constructed a H_2/hydride//perovskite/O_2 alkaline fuel cell to evaluate how the AB_5-type hydrogen storage alloys can be used as catalysts in the hydrogen-diffusion electrodes. The results showed that a maximum power density of 54 mW/cm^2 was achieved at 120 mA/cm^2 using H_2/O_2 and 49 mW/cm^2 at 100 mA/cm^2 when using H_2/air. The hydrogen- and oxygen-diffusion electrodes showed stable performance and life-tests. The catalytic activities, stability, and power densities could be further improved if much smaller hydride particles could be developed as catalysts in the hydrogen-diffusion electrodes. In addition, we also observed no noticeable difference in the activity between pure H_2 and a 10−25 ppm CO-containing H_2 when using this kind of AB_5-type hydrogen storage alloy electrode.

References and Notes

(1) Kordesch, K. V.; Simader, G. *Chem. Rev.* **1995**, *95*, 191.
(2) Berger, D. J. *Science* **1999**, *286*, 49.
(3) Appleby, A. J. *Sci. Am.* **1999**, *281*, 74.
(4) Wang, X. H.; Chen, Y.; Pan, H. G.; Xu, R. G.; Li, S. Q.; Chen, L. X.; Chen, C. P.; Wang, Q. D. *J. Alloys Compd*. **1999**, *293*−*295*, 833.
(5) Chartouni, D.; Kuriyama, N.; Kiyobayashi, T.; Chen, J. *Int. J. Hydrogen Energy* **2002**, *27*, 945.
(6) Hu, W. K.; Noréus, D. *J. Alloys Compd*. **2003**, *356*−*357*, 734.
(7) Bursell, M.; Pirjamali, M.; Kiros, Y. *Electrochim. Acta* **2002**, *47*, 1651.
(8) Kiros, Y. WO 2002075827.
(9) Willems, J. J. G.; Buschow, K. H. *J. Less-Common Met*. **1987**, *129*, 13.
(10) Durairajia, A.; Haran, B. S.; White, R. E.; Popov, B. N. *J. Power Sources* **2002**, *87*, 84.
(11) Kiros, Y.; Schwartz, S. *J. Power Sources* **2000**, *87*, 101.
(12) Mohamedi, M.; Sato, T.; Itoh, T.; Umeda, M.; Uchida, I. *J. Electrochem. Soc.* **2002**, *149*, A983.
(13) Macpherson, J. V.; Unwin, P. R. *Anal. Chem.* **1997**, *69*, 2063.
(14) Simons, J. W.; Flanagan, T. B. *J. Phys. Chem*. **1965**, *69*, 3581.
(15) Lin, T. S.; Gomer, R. *Surf. Sci*. **1991**, *255*, 41.
(16) Meli, F.; Schlapbach, L. *J. Less-Common Met*. **1991**, *174*, 1252.
(17) Lemons, R. A. *J. Power Sources* **1990**, *29*, 251.
(18) Gottesfeld, S.; Zawodzinski, T. A. *Adv. Electrochem. Sci. Eng*. **1997**, *5*, 195.
(19) Acres, G. J. K.; Frost, J. C.; Hards, G. A.; Potter, R. J.; Ralph, T. R.; Thompsett, D.; Burstein, G. T.; Hutchings, G. J. *Catal. Today* **1997**, *38*, 393.
(20) Hammer, B.; Nielsen, O. H.; Noerskov, J. K. *Catal. Lett.* **1997**, *46*, 31.
(21) Divisek, J.; Oetjen, H. F.; Peinecke, V.; Schmidt, V. M.; Stimming, U. *Electrochim. Acta* **1998**, *43*, 3811
(22) Gasteiger, H. A.; Markovic, N. M.; Ross, P. N. *J. Phys. Chem.* **1995**, *99*, 8945.